PAPER • OPEN ACCESS

Neutrino-nucleus reactions on oxygen and neon for nucleosynthesis and supernova neutrino detection

To cite this article: Toshio Suzuki et al 2020 J. Phys.: Conf. Ser. 1643 012027

View the <u>article online</u> for updates and enhancements.



1643 (2020) 012027

doi:10.1088/1742-6596/1643/1/012027

Neutrino-nucleus reactions on oxygen and neon for nucleosynthesis and supernova neutrino detection

Toshio Suzuki^{1,2}, Satoshi Chiba³, Takashi Yoshida⁴, Ken'ichiro Nakazato⁵, Makoto Sakuda⁶, Koh Takahashi⁷ and Hideyuki Umeda³

suzuki@phys.chs.nihon-u.ac.jp

Abstract. Spin-dipole strength in ^{16}O and v-induced reactions on ^{16}O are studied by shell-model calculations. Charged- and neutral-current reaction cross sections for various particle and γ emission channels as well as the total ones are evaluated with the Hauser-Feshbach statistical method. Nucleosynthesis of ^{11}B and ^{11}C in supernovae through αp emission channels is investigated. Charged-current reaction cross sections induced by supernova ν and their dependence on ν oscillations are discussed for future supernova burst. Neutrino-nucleus reaction cross sections on ^{20}Ne induced by Gamow-Teller and spin-dipole transitions are also investigated. Electron-capture rates for the forbidden transition ^{20}Ne (e^- , ν_e) ^{20}F ($2_{g.s.}^{-+}$) at stellar environments are discussed.

1. Introduction

Roles of Gamow-Teller (GT) transitions in nuclear rates, electron-capture and β -decay rates at stellar environments, have been investigated in various astrophysical processes [1-5]. Neutrino-nucleus reaction cross sections for ^{12}C [6,7], ^{13}C [8], ^{40}Ar [9], ^{56}Fe and ^{56}Ni [10] have been updated, and applied to study v-process nucleosynthesis [6,7,11] and v properties [7,11]. Here, we discuss forbidden transitions in ^{16}O . Spin-dipole strengths in ^{16}O and v-induced reactions on ^{16}O are studied in Sect. 2. Partial cross sections in various channels including multi-particle emissions are evaluated by the Hauser-Feshbach method, and implications on nucleosynthesis of light elements in supernovae are discussed. Effects of v oscillations on charged-current reaction cross sections for supernova v are investigated. In Sect. 3, v-induced reactions on ^{20}Ne , in which both the GT and spin-dipole contributions are important, are studied. Electron-capture rates for a second-forbidden transition in ^{20}Ne are evaluated with the multipole expansion method.

Published under licence by IOP Publishing Ltd

¹Department of Physics, College of Humanities and Sciences, Nihon University, Sakurajosui 3, Setagaya-ku, Tokyo 156-8550, Japan.

²National Astronomical Observatory of Japan, Mitaka, Tokyo 181-8588, Japan

³Research Laboratory for Nuclear Reactors, Tokyo Institute of Technology, Meguroku, Tokyo 152-8550, Japan

⁴Department of Astronomy, Graduate School of Science, The University of Tokyo, Tokyo 113-0033, Japan

⁵Faculty of Arts & Science, Kyushu University, 744 Motooka, Nishi-ku, Fukuoka 819-0395, Japan

⁶Department of Physics, Okayama University, 3-1-1 Tsushimanaka, Kita-ku, Okayama 700-8530 Japan

⁷Max-Planck-Institut für Gravitationsphysik (Albert Einstein Institute), Am Muhlenberg 1, D-14476, Potsdam-Golm, Germany

Content from this work may be used under the terms of the Creative Commons Attribution 3.0 licence. Any further distribution of this work must maintain attribution to the author(s) and the title of the work, journal citation and DOI.

1643 (2020) 012027

doi:10.1088/1742-6596/1643/1/012027

2. v-induced reactions on ¹⁶O

2.1. Spin-dipole strength in ¹⁶O

v-induced reactions on 12 C was studied with a shell-model Hamiltonian, SFO [15], which can reproduce the GT strength in 12 C and magnetic moments of p-shell nuclei systematically. The configuration space of the SFO is p-sd shell, and the quenching factor for $q = g_A^{eff}/g_A$ is found to be close to 1, q = 0.95, in contrast to the case within p-shell configurations such as the Cohen-Kurath Hamiltonian [16]. The monopole term in spin-isospin flip channel is enhanced in the SFO.

In the case of 16 O, the GT strength is small and the spin-dipole strength is the dominant contribution to spin-dependent transitions. Therefore, the p-sd cross-shell matrix elements in SFO are improved by taking into account the tensor and two-body spin-orbit components properly: the tensor and two-body spin-orbit components are replaced by those of π + ρ meson-exchanges and σ + ρ + ω meson-exchanges, respectively. A new Hamiltonian thus obtained, SFO-tls [17], can reproduce low-lying energy levels of spin-dipole states in 16 O. Calculated spin-dipole strength

$$B(SD\lambda)_{\mp} = \frac{1}{2J_i + 1} \sum_{f} |\langle f || S_{\mp}^{\lambda} || i \rangle|^2$$

$$S_{\mp\mu}^{\lambda} = r[Y^1 \times \vec{\sigma}]_{\mu}^{\lambda} t_{\mp}$$
(1)

in 16 O for $\lambda^{\pi} = 0^{-}$, 1^{-} and 2^{-} are shown in figure 1. Here, J_i is the initial spin, and $t_-|n\rangle = |p\rangle$ and $t_+|p\rangle = |n\rangle$.

Sum value $B(SD\lambda)$ is nearly proportional to $2\lambda+1$, while the averaged energy position is the lowest (highest) for 2^- (1^-). The latter can be explained by using the energy-weighted sum (EWS) of the strength. For LS-closed core, the EWS splits for different λ due to one-body spin-orbit interaction. Two-body tensor interaction affects it further; it is attractive for 2^- and 0^- while repulsive for 1^- (see Ref. [18] for the details).

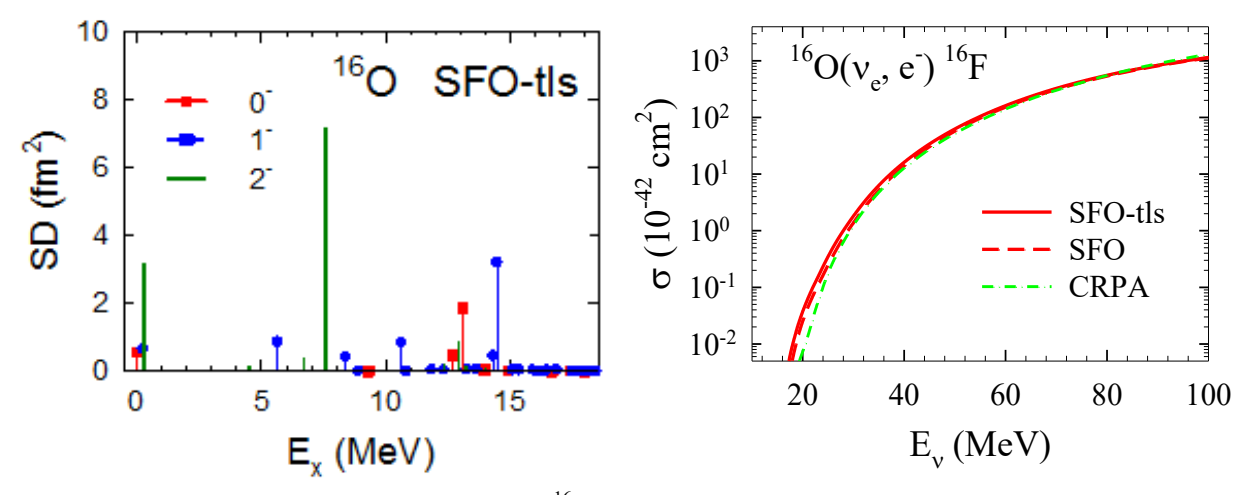


Figure 1. Calculated spin-dipole strength in ¹⁶O obtained with the SFO-tls. (Taken from Ref. [18])

Figure 2. Calculated total cross sections for 16 O (v_e , e^-) 16 F obtained by shell-model calculations with the SFO-tls and SFO as well as CRPA calculation [21]. (Taken from Ref. [18])

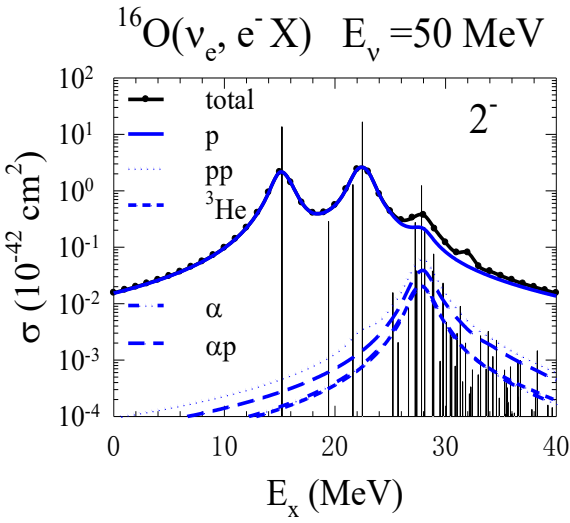
2.2 ν -induced cross sections on ^{16}O

Charged- and neutral-current v-nucleus reaction cross sections on ^{16}O are evaluated by shell-model calculations with the SFO-tls [18]. The quenching for g_A is taken to be q=0.95. The total μ -capture rate on ^{16}O obtained with q=0.95 is λ = 11.20×10⁴ s⁻¹ (10.21×10⁴ s⁻¹) for SFO-tls (SFO), which is close to the experimental value, λ = 11.26×10⁴ s⁻¹ [20]. Total charge-exchange cross sections for ^{16}O (v_e , e^-)

1643 (2020) 012027

doi:10.1088/1742-6596/1643/1/012027

 ^{16}F at E_{ν} < 100 MeV obtained for SFO-tls as well as for SFO and previous continuum-random-phase approximation (CRPA) calculation [21] are shown in figure 2. The multipolarities up to J=4 are taken into account. Dominant contributions come from the transitions with $J^{\pi}=2^{-}$ and 1^{-} . The cross sections for SFO-tls are enhanced compared with those of SFO, and found to be close to those of the CRPA except at E_{ν} < 30 MeV. Neutral-current cross sections for SFO-tls are also close to those of the CRPA.



 E_x (MeV) **Figure 3a.** Calculated partial cross sections for 16 O (v_e , e^- X) with X = p, pp, 3 He, α , αp , via excitations of 2^- states in 16 F obtained by shell-model calculation with the SFO-tls. (Taken from Ref. [18])

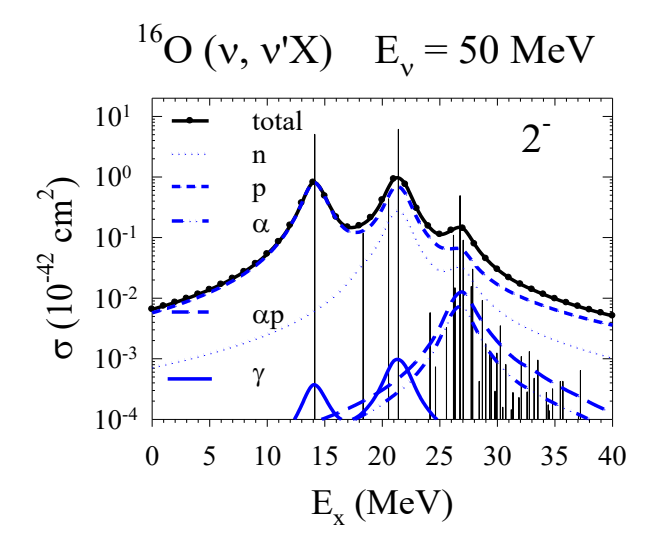


Figure 3b. The same as in figure 3a for neutralcurrent reaction $^{16}O(v, v'X)$ with $X=n, p, \alpha, \alpha p$ and γ via excitations of 2^- states in ^{16}O . (Taken from Ref. [18])

Partial cross sections for various particle and γ emission channels, including multi-particle emissions in addition to single-particle ones, are evaluated by the Hauser-Feshbach method. Charged-current cross sections for p, pp, 3 He, α and α p emission channels for the excitations of 2^- states are shown in figure 3a for SFO-tls. The proton emission channel gives the dominant contribution, while α p and α emission channels become important at higher excitation energies at $E_x \sim 30$ MeV. A large branching ratio for the α p channel leads to the production of 11 B and 11 C by 16 O (ν , ν ' α p) 11 B and 16 O (ν e, $e^-\alpha$ p) 11 C reactions, respectively, in addition to the ordinary reaction channels 12 C (ν , ν 'p) 11 B and 12 C (ν e, e^- p) 11 C. The production yields of 11 B + 11 C in supernovae with 15 (20) M_{\odot} are found to be enhanced by about 13 (12)% compared with those without the multi-particle emission channels [18] (see table 1).

Table 1. Production yields of ¹¹B and ¹¹C in superrnova explosion for progenitor mass of M=15M $_{\odot}$. Here, "single-particle channels" denotes γ , p, n and α emission channels.

Production yield $(10^{-7} \mathrm{M}_{\odot})$	HW92 Single-particle channels	SFO-tls Single-particle channels	SFO-tls Single+Multi- particle channels
¹¹ B	2.94	2.92	3.13.
¹¹ C	2.80	2.71	3.20
¹¹ B+ ¹¹ C	5.74	5.62	6.33

1643 (2020) 012027

doi:10.1088/1742-6596/1643/1/012027

2.3 v oscillations and detection of supernova v

The MSW matter resonance oscillations [22] occur in C-He layer of supernovae for normal (inverted) mass hierarchy in charged-current reactions induced by $v_e(\overline{v}_e)$. Event spectra of neutrino- ^{16}O charged-current reactions at Super-Kamiokande are evaluated for future supernova neutrino bursts. The cross sections of the ^{16}O (v_e , e^-) X and ^{16}O (\overline{v}_e , e^+) X reactions for each nuclear state with a different excitation energy are evaluated, and dependence of the cross sections on the mass hierarchies are examined [23]. Enhancement of expected event numbers for supernovae with mass of $20M_\odot$ at 10~kpc away from the earth is predicted for the v_e and $\overline{v}_e(\overline{v}_e)$ -induced reaction in case of normal (inverted) hierarchy. In case of supernovae with mass of $30M_\odot$ corresponding to black hole formation model, enhancement of the event numbers is unremarkable due to less total emission energies for v_x and \overline{v}_x (x = μ , τ) compared with v_e and \overline{v}_e . However, event numbers of the main background, the inverse β decay, are suppressed compared with the supernova events at higher energy e^+/e^- region (see Ref. [23] for more details).

3. v-induced reactions on ²⁰Ne

3.1 GT strength in ²⁰Ne and reaction cross sections

Neutrino- 20 Ne reactions, 20 Ne (v, v'p) 19 F and 20 Ne (\overline{v}_e e⁺) 20 F followed by neutron emission, lead to production of 19 F. First, we study GT strength in 20 Ne by shell-model calculations with the use of various Hamiltonians, USDB (sd) [24], WBP (p-sd-pf) [25], YSOX (p-sd) [26] and SFO-tls (p-sd). Here, shell-model configuration spaces for the Hamiltonians are denoted in the parentheses. Calculated cumulative sums of the strength are shown in figure 4 as well as the experimental data obtained by (p, n) and (n, p) reactions [27]. If factor q=0.90 and SFO-tls with q =0.95 are continuous to obtain the v-induced reaction continuous to ob

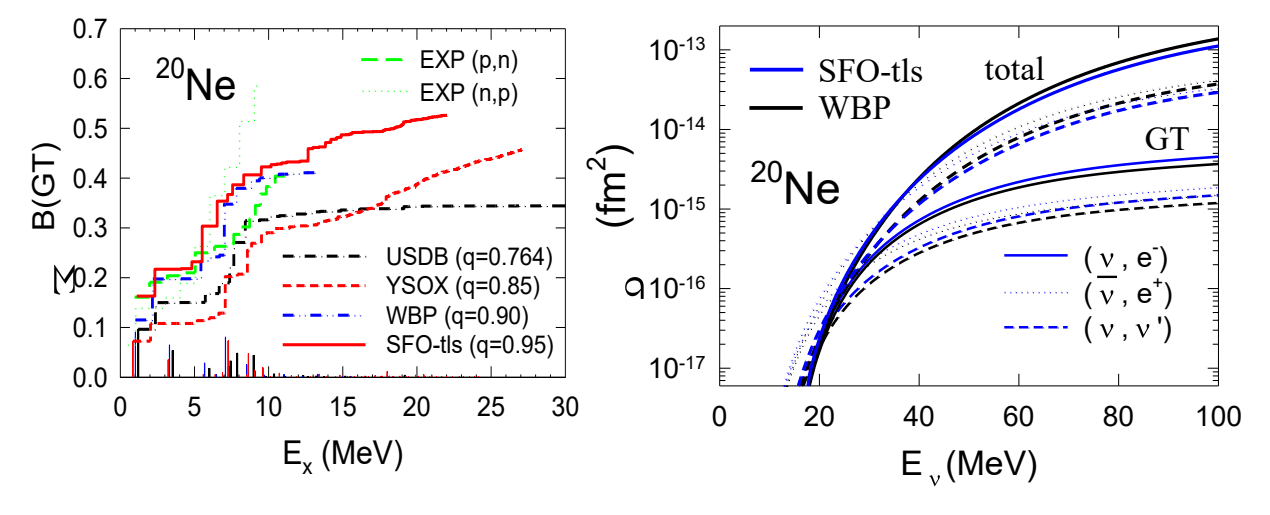


Figure 4. Cumulative sums of the GT strengths in 20 Ne obtained with USDB, WBP, YSOX and SFO-tls using the quenching factor q for g_A . Experimental data from (n, p) and (p, n) reactions [27] are also shown.

Figure 5. Calculated total cross sections for (v, e^{-}) , $(\overline{v}_{e}, e^{+})$ and (v, v') reactions on 20 Ne obtained with the WBP (q=0.90) and SFO-tls (q=0.95). The cross sections for the GT transitions only and those for all the multipolarities are shown.

1643 (2020) 012027

doi:10.1088/1742-6596/1643/1/012027

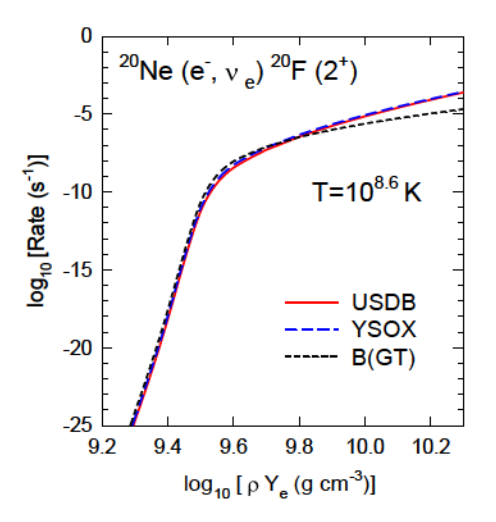
As the Q value for $(\overline{\nu}_e, e^+)$ is the lowest, the $(\overline{\nu}_e, e^+)$ cross sections are the largest among them at low ν energies. Cross sections for the GT transitions with the SFO-tls are larger than those with the WBP. Contributions from the spin-dipole transitions become more important than the GT ones at $E_{\nu} > 30$ MeV. Total cross sections for the WBP become larger than those for the SFO-tls at $E_{\nu} > 30$ MeV as the configuration space for the WBP is larger than that for the SFO-tls, while the difference is moderate. Evaluations of partial cross sections for particle and γ emission channels that are important for the production of ^{19}F are in progress.

3.2 Electron-capture rates on ²⁰Ne

We discuss electron-capture rates for a second-forbidden transition 20 Ne $(0_{g.s.}^+) \rightarrow ^{20}$ F $(2_{g.s.}^+)$. This transition is triggered first for 20 Ne (\overline{v}_e, e^+) 20 F, but the contribution from the transition is small and almost negligible at low E_v . On the other hand, at high densities the forbidden transition becomes dominant in the e-capture reaction on 20 Ne [28].

dominant in the e-capture reaction on 20 Ne [28]. Recently, the β -decay rate for the transition 20 F ($2_{g.s.}^+$) \rightarrow 20 Ne ($0_{g.s.}^+$) was measured, and $\log ft$ value was obtained to be 10.89±0.11 [29]. Here, we evaluate the e-capture rates with the multipole expansion method [30]. In this method, there are contributions from the Coulomb, longitudinal, transverse electric and axial magnetic terms with the multipolarity $J^{\pi} = 2^+$. The transition strength has a dependence on the electron energy in contrast to the allowed GT transition. Calculated e-capture rates for the forbidden transition obtained with the USDB and YSOX Hamiltonians are shown in figure 6 for the temperature $\log_{10}T = 8.6$. Effects of the Coulomb effects, that is, the screening effects on both electrons and ions [31-34] are also investigated. Results obtained by the prescription assuming an allowed GT transition with the strength determined from the experimental $\log ft$ value (=10.89) are also shown for comparison. Sizable difference is found between the two methods [35], which comes from the difference in the electron energy dependence of the transition strengths between the two methods. The $\log ft$ value for the β -decay transition 2^0 F ($2_{g.s.}^+$) \rightarrow 2^0 Ne ($0_{g.s.}^+$) is obtained to be $\log ft = 11.18$ and 11.24 for the USDB and YSOX, respectively, with the present multipole expansion method [35]. These values are consistent with the experimental value within a factor of ~ 2 .

Heating of the O-Ne-Mg core due to γ emissions succeeding the double e-capture reactions, ²⁰Ne (e⁻, v_e) ²⁰F (e⁻, v_e) ²⁰O, is important in the final stage of the evolution of the core. Study of the evolution of the high density electron-degenerate core with the use of the present shell-model rates is in progress [36].



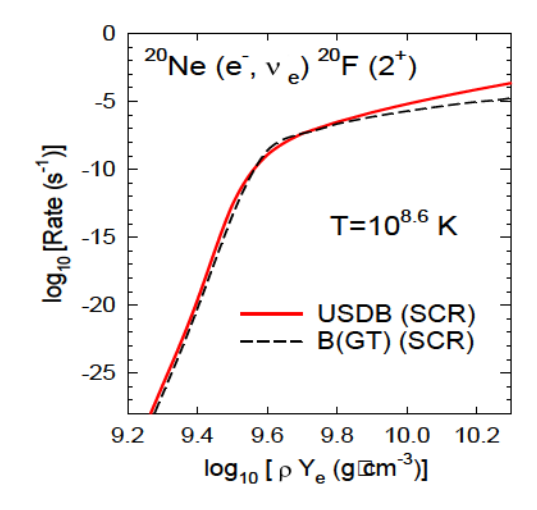


Figure 6. Electron-capture rates for the forbidden transition 20 Ne (e⁻, ν_e) 20 F ($2_{g.s.}^+$) at T =10^{8.6} (K) obtained by shell-model calculations with the USDB and YSOX. The rates obtained by the prescription assuming an allowed GT transition are also shown. In the right panel, the Coulomb effects (SCR effects of electron and ion) are included.

1643 (2020) 012027

doi:10.1088/1742-6596/1643/1/012027

The authors would like to thank K. Nomoto, S. Zha and S.-C. Leung for useful discussions and studies on the evolution of the O-Ne-Mg core. This work has been supported in part by JSPS KAKENH Grant Nos. JP15K05090 and JP19K03855. K.T. was supported by the JSPS Overseas Research Fellowships.

References

- [1] Suzuki T, Toki H and Nomoto K 2016 ApJ 817,163
- [2] Toki H, Suzuki T, Nomoto K, Jones S and Hirschi R 2013 Phys. Rev. C 88 015806
- [3] Jones S, Hirschi R, Nomoto K et al. 2013 ApJ 772 150
- [4] Honma M, Otsuka T, Mizusaki T, Hjorth-Jensen M and Brown B A 2005 JPhCS 20 7
- [5] Mori K, Famiano M, Kajino T, Suzuki T et al. 2016 *ApJ* **833** 179
- [6] Suzuki T, Chiba S, Yoshida T, Kajino T and Otsuka T 2006 Phys. Rev. C 74 034307
- [7] Yoshida T, Suzuki T, Chiba S, Kajino T et al. 2008 *ApJ* **686** 448
- [8] Suzuki T, Balantekin A B and Kajino T 2012 Phys. Rev. C 86 015502
- [9] Suzuki T and Honma M 2013 Phys. Rev. C 87 014607
- [10] Suzuki T, Honma M, Higashiyama K, Yoshida T, Kajino T, Otsuka T, Umeda H and Nomoto K 2009 *Phys.Rev. C* **79** 061603
- [11] Suzuki Tand Kajino T 2013 J. Phys. G 40 083101
- [12] Möller P, Nix J R and Kratz K-L 1997 ADNDT 66 131 Möller P, Pfeiffer B and Kratz K-L 2003 Phys. Rev. C 67 055802
- [13] Suzuki T, YoshidaT, KajinoT and Otsuka T 2012 Phys. Rev. C 85 015802
- [14] Suzuki T, Shibagaki S, Yoshida T, Kajino T and Otsuka T 2018 ApJ 859 133
- [15] Suzuki T, Fujimoto R and Otsuka T 2003 Phys. Rev. C 67 044302
- [16] Cohen S and Kurath D 1965 Nucl. Phys. 73 1
- [17] Suzuki T and Otsuka T 2008 Phys. Rev. C 78 061302
- [18] Suzuki T, Chiba S, Yoshida T, Takahashi K and Umeda H 2018 Phys. Rev. C 98 034613
- [19] Suzuki T and Sagawa H 1998 Nucl. Phys. A 637 547
- [20] Suzuki T, Measday D F and Roalsvig J P 1987 Phys. Rev. C 35 2212
- [21] Langanke K, Vogel P and Kolbe E 1996 *Phys. Rev. Lett.* **76** 2629 Kolbe E, Langanke K and Vogel P 2002 *Phys. Rev. D* **66** 013007
- [22] Wolfenstein L 1978 Phys. Rev. D 17 2369; 1979 Phys. Rev. D 20 2634
 Mikheyev S P and Smirnov A Y 1985 Sov. J. Nucl. Phys. 42 913
- [23] Nakazato K, Suzuki T and Sakuda M 2018 PTEP 2018 123E02
- [24] Brown B A and Richter W A 2006 *Phys. Rev. C* **74** 034315 Richter W A, Mkhize S and Brown B A 2008 *Phys. Rev. C* **78** 064302
- [25] Warburton E K and Brown B A 1992 *Phys. Rev. C* **46** 923
- [26] Yuan C, Suzuki T, Otsuka T, Xu F and Tsunoda N 2012 Phys. Rev. C 85 064324
- [27] Pointon B W et al. 1991 Phys. Rev. C 44 2430; Anderson B D 1991 Phys. Rev. C 43 50
- [28] Martinez-Pinedo G, Lam Y H, Langanke K, Zegers R G and Sullivan C 2014 *Phys. Rev. C* **89** 045806
- [29] Riisager K 2019 talk at INPC2019 Kirsebom O S et al. 2018 arXiv:1805.08149; 2019 arXiv:1905.09407
- [30] O'Connell J S, Donnelly T W and Walecka J D 1972 *Phys. Rev. C* **6** 719 Walecka J D in *Muon Physics*, edited by Hughes V M and Wu C S (Academic Press, New York, 1975), pp. 113-218; Parr N, Colo G, Khan E and Vretenar D 2009 *Phys. Rev. C* **80** 055801
- [31] Itoh N, Tomizawa N, Tamamura M and Wanajo S 2002 ApJ 579 380
- [32] Ichimaru S 1993 Rev. Mod. Phys. 65 255
- [33] Slattery W L, Doolen G D and DeWitt H E 1982 Phys. Rev. A 26 2255
- [34] Juodagalvis A, Langanke K, Hix W R, Martinez-Pinedo G and Sampaio J M 2010 *Nucl. Phys. A* **848** 454
- [35] Suzuki, Zha S, Leung S-C and Nomoto K 2019 ApJ 881 64
- [36] Zha S, Leung S-C, Suzuki T and Nomoto K 2019 *ApJ* submitted, arXiv:1907.04184 (2019)